

Twist Angle, Strain, Broken Rotational Symmetry, Corrugation and Supercell in Twisted Bilayer Graphene

Veerpal¹ and Ajay²

Department of Physics, Indian Institute of Technology Roorkee^{1,2}

E-mail: veerpal@ph.iitr.ac.in¹ and ajay@ph.iitr.ac.in²

Abstract. This work put forward a comprehensive study of moire pattern in commensurate twisted bilayer graphene (TBG) to determine the connection of moire period with corresponding twist angle. Using the understanding of moire pattern, computational codes are developed to simulate the planar positions of carbon atoms lying in a large specimen of commensurate twisted bilayer graphene (CTBG) with any commensurate twist angle. With the help of simulated moire patterns of CTBG it is demonstrated that for many commensurate twist angles the apparent moire period may be quite different from the actual moire period, and the same moire pattern may have multiple slightly different values of the apparent moire period. These multiple slightly different values of the apparent moire period show that strain and broken rotational symmetry in moire pattern of CTBG are intrinsic. From various values of apparent moire period, the apparent strain in moire pattern of CTBG is calculated for many commensurate twist angles; the calculated values of apparent strain are in good agreement with experimentally reported values. Taking some insight from available experimental data related to twisted bilayer graphene systems and conventional bilayer graphene systems, corrugation in CTBG is modelled and incorporated with the simulated positions of carbon atoms. Thus, simulated corrugated CTBG system resembles with actual corrugated TBG systems. There is a pattern in positions of superlattice points of moire pattern in CTBG. Using the positions of superlattice points and some simple concepts of geometry, some logics are constructed to computationally extract positions of carbon atoms lying inside a supercell from a computationally simulated large specimen of CTBG. Using these logics very efficient computational codes are written to simulate the positions of carbons atoms lying inside a supercell of CTBG and positions of carbon atoms lying inside a supercell of CTBG are simulated.

1. Introduction

Graphene based layered materials with a relative twist between the layers possess many interesting properties e.g., moire pattern in their lattice structure, flat band near Dirac point[1, 2], Van-Hove singularities near Fermi level[3, 4, 5], unconventional superconductivity[6, 7, 8], correlated insulator behaviour[9], anomalous Hall effect at half filling[10], ferromagnetism[11, 12], Hofstadter butterfly[13] and many more.

Electronic properties of TBG systems change with twist angle and filling factor (number of electrons per supercell); therefore, these electronic properties are attributed to evolution of interlayer interaction driven by change in moire pattern dependent on twist angle along with electronic correlation[4, 14, 5] effects dependent on carrier density. Ideal moire patterns of TBG are assumed to be defect free but experimentally observed moire patterns of TBG show presence of defects such as strain and broken rotational symmetry[5, 4, 14, 15]. These defects also affect the electronic properties of TBG systems. It is proposed [6, 8] that investigation of electronic correlations in twisted bilayer graphene (TBG) may be helpful in solving the mystery of high temperature superconductivity, as well as it can help to understand other electronic correlations-based effects. This hope is motivating scientific community to study the theoretical and experimental aspects of these materials more rigorously. Currently the of experimental studies related to TBG have advanced significantly but despite the great motivation, the theoretical studies of these materials needed to understand electronic correlations are still lagging. There are some issues which are causing this lag. Due to large number (of the order of 10000) of carbon atoms in a moire supercell of TBG and lack of technique to process internal configuration of carbon atoms inside a moire supercell; incorporation of the complete lattice structure of moire supercell in quantum mechanical calculations is still missing. Physical understanding and quantum mechanical treatment of interlayer-coupling and electronic-correlations still needs improvements. Exact reasons behind defects in moire pattern of TBG are still not very clear. There are many research papers[16, 17, 18, 19, 20] which provide very good description of commensurate moire pattern and report the relation between commensurate moire period L_c and commensurate twist angle θ_c in CTBG, but there is a scope for improvement of this description. The work presented here offer a comprehensive study of structure of CTBG and show that strain and rotational symmetry breaking appearing in TBG systems can appear due to intrinsic reasons. This work also offers mathematical model to incorporate corrugation in structure of TBG along with a technique to determine internal configuration of carbon atoms inside a moire supercell of TBG. Using the logics presented here computational codes can be written which can be so efficient that internal configuration of carbon atoms inside a moire supercell of TBG can be simulated within few minutes even on a laptop with moderate computing power.

The content of following sections in this paper is organized as follows. In Sec. 2, we comprehensively discuss logics determining the relation of commensurate moire period with corresponding commensurate twist angle. In Sec. 3, we discuss intrinsic reasons causing strain and rotational symmetry breaking. In Sec. 4, we discuss logics to incorporate corrugation in structure of TBG. In Sec. 5, we discuss logics to develop techniques for determination of internal configuration of carbon atoms inside a moire supercell of TBG. In Sec. 6, we make conclusion.

2. Relation between moire period and twist angle in TBG

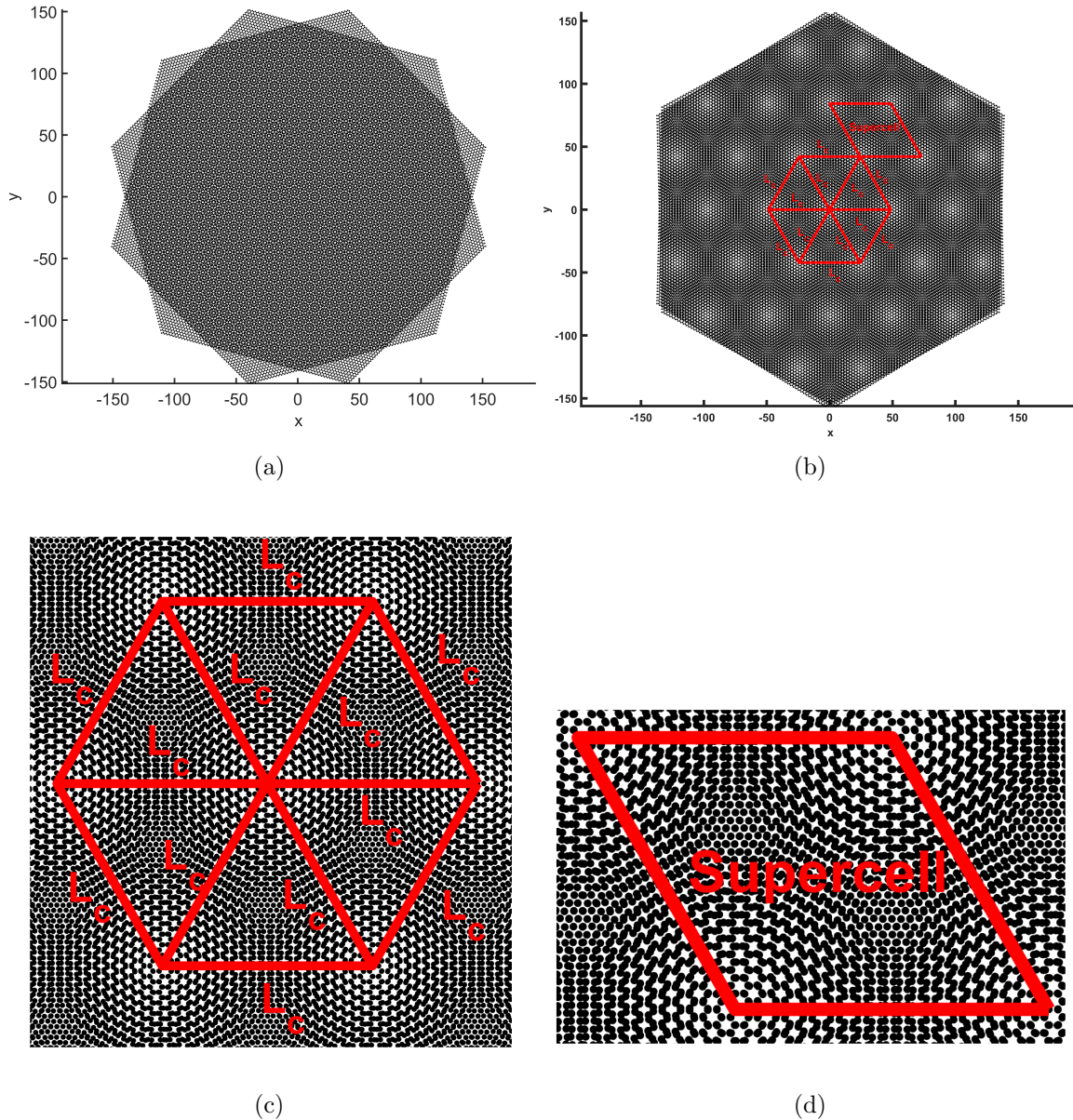


Figure 1: (a) Incommensurate moire pattern in TBG corresponding to twist angle= 30° , (b) commensurate moire pattern, (c) moire period L_c and (d) supercell in TBG corresponding to twist angle= 2.876° (viewed from top)

To develop theoretical formulation for TBG, it is essential to properly understand the lattice structure of moire pattern in TBG. The observed moire patterns in TBG systems are categorized in two categories: incommensurate moire patterns^{1a} and commensurate moire patterns^{1b}. Commensurate moire patterns possess perfect periodicity while incommensurate moire patterns lack in perfect periodicity. Due to perfect periodicity of commensurate moire patterns, the quantum mechanical

calculations needed to calculate the electronic properties of the infinitely large twisted bilayer graphene can be reduced to the supercell of finite size.

For observed commensurate moire patterns the scale of periodicity (superlattice constant or moire period L_c) is generally very large as compared to scale of periodicity (lattice constant of graphene denoted by $a_o = a\sqrt{3} \approx 2.45 \text{ \AA}$) in conventional bilayer graphene. To calculate electronic properties of twisted bilayer graphene we need to deal with moire supercell containing very large number of atoms (of the order of 10000) equal to $N_s = 4L_c^2$ (here L_c is in units of a_o). The lattice structure of moire pattern in twisted bilayer graphene can be considered to be modified form of conventional bilayer graphene (either AA-stacked or AB-stacked bilayer graphene) after introducing relative twist between the two layers. Conventional bilayer graphenes are composed of

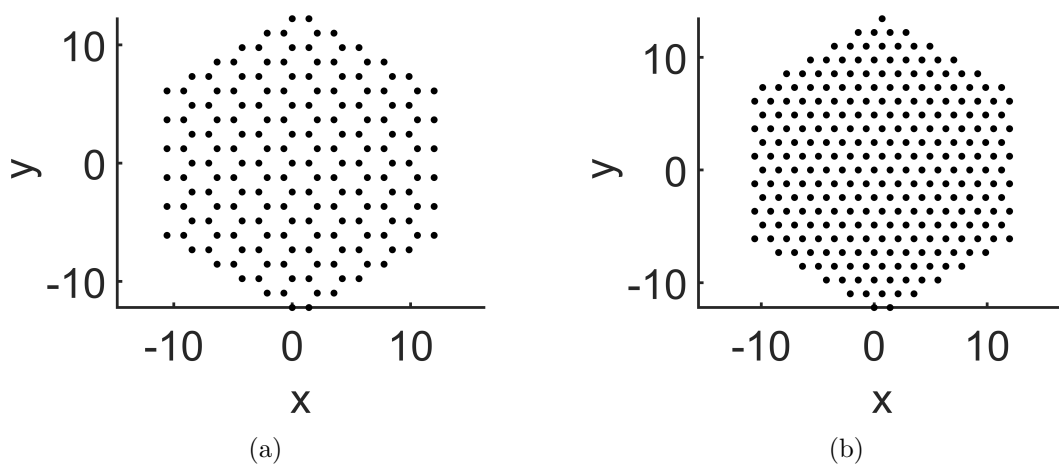


Figure 2: (a) Position of carbon atoms in AA-stacked bilayer graphene and monolayer graphene, (b) Position of carbon atoms in AB-stacked bilayer graphene (viewed from top)

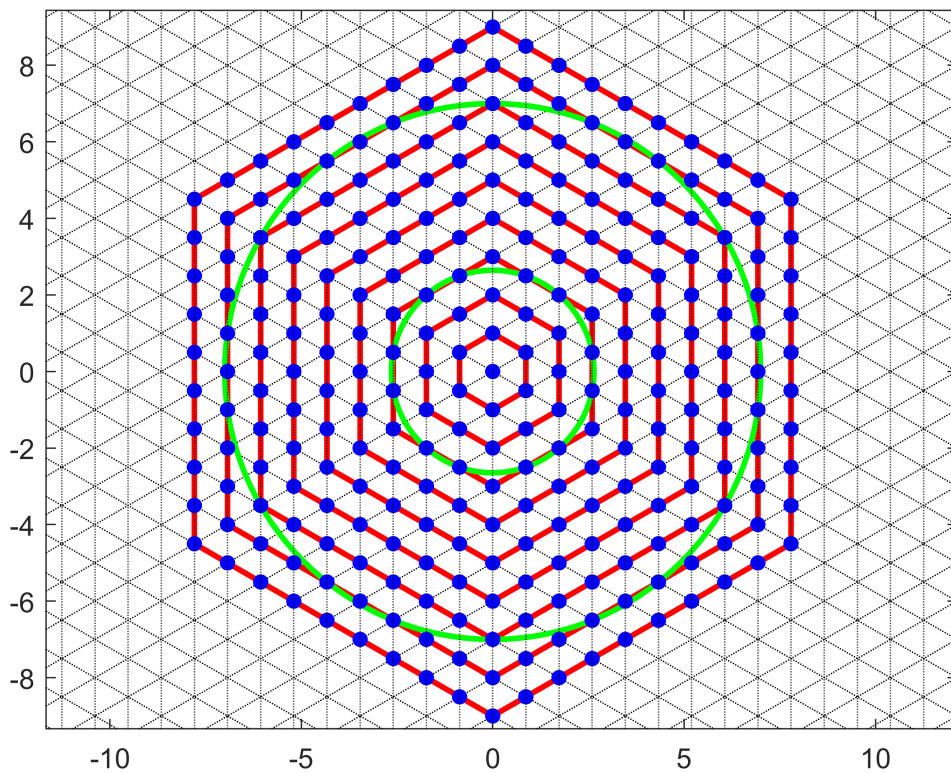
graphene. In Graphene[21] carbon atoms are arranged on a honeycomb structure made from hexagons and show sp^2 hybridization, hence forming a planar structure. The distance between two carbon atoms is $a \approx 1.415 \text{ \AA}$. The sigma bonds in the hexagonal network strongly connect the carbon atoms. These sigma bonds create the planar honeycomb lattice structure of graphene. The non-hybridized p_z orbitals of carbon atoms which are perpendicular to the planar structure, contain one electron each. These electrons of p_z orbitals, can move from one p_z orbital to other neighbouring p_z orbital. Dynamics of these electrons of p_z orbitals, driven by the influence other electrons, lattice structure, external field, temperature etc., decide the electronic properties of graphene-based materials. Lattice structure of graphene can be considered to possess two interpenetrating triangular lattices denoted as A and B sublattices, and each sublattice point is occupied by one carbon atom. The two sublattices in graphene are described by same Bravais lattice vectors $\mathbf{a}_1 = \frac{a_o}{2}(\sqrt{3}\hat{x} + \hat{y})$ and $\mathbf{a}_2 = \frac{a_o}{2}(\sqrt{3}\hat{x} - \hat{y})$ but they have different translation vectors to neighbours. Angle between \mathbf{a}_1 and \mathbf{a}_2 is 60° . For same triangular

lattice one can also choose basis vectors which have 120° angle between them. Here a_o ($= 2.46\text{\AA}$) is the lattice constant for graphene. Corresponding reciprocal lattice basis vectors are $\mathbf{b}_1 = \frac{2\pi}{a_o\sqrt{3}}(\hat{k}_x + \sqrt{3}\hat{k}_y)$; $\mathbf{b}_2 = \frac{2\pi}{a_o\sqrt{3}}(\hat{k}_x - \sqrt{3}\hat{k}_y)$ which create a hexagonal first Brillouin zone. The Corners of the first Brillouin zone of graphene are known as Dirac point because near Dirac point the electrons behave as relativistic Dirac particles showing linear dispersion in graphene. Coordinates of Dirac points \mathbf{K} and \mathbf{K}' are given as $\mathbf{K} = \frac{2\pi}{a_o\sqrt{3}}(1, \frac{1}{\sqrt{3}})$ and $\mathbf{K}' = \frac{2\pi}{a_o\sqrt{3}}(1, \frac{-1}{\sqrt{3}})$.

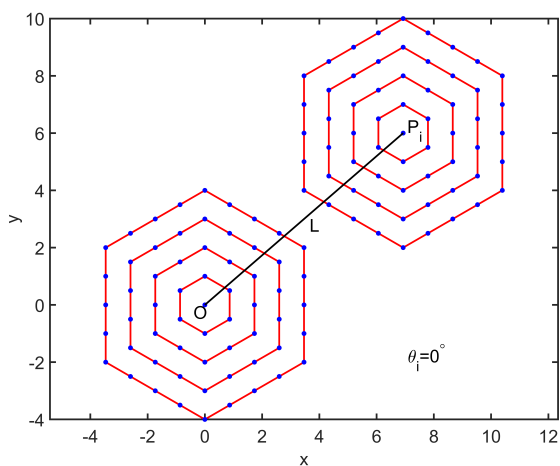
Let A_1, B_1 denote sublattices of lower layer and A_2, B_2 denote sublattices of upper layer. The conventional bilayer graphene has two graphene layers, one layer (consider it to be 2^{nd} layer) stacked on top of other layer (consider it to be 1^{st} layer). In AA-stacked bilayer graphene planar positions of A_1 sublattice coincide with planar positions of A_2 sublattice and planar positions of B_1 sublattice coincide with planar positions of B_2 sublattice. In AB-stacked bilayer graphene planar positions of A_1 sublattice coincide with planar positions of B_2 sublattice but planar positions of B_1 sublattice do not coincide with planar positions of A_2 sublattice. In conventional bilayer graphene distance between two graphene planes is uniform everywhere, this inter-layer distance is $d_{\perp AB} = 3.35\text{\AA}$ [22] in AB-stacked bilayer graphene and $d_{\perp AA} = 3.55\text{\AA}$ [23] in AA-stacked bilayer graphene. In both the cases planar positions of at least one sublattice of lower layer coincides with planar positions of one sublattice of upper layer. The origin can be considered to be situated at planar position of one of the coinciding sublattice points (A_1 or A_2 in AA-stacked bilayer graphene and A_1 or B_2 in AB-stacked bilayer graphene). When a layer (consider it to be the upper layer) is rotated (or twisted) with respect to other layer (consider it to be the lower layer) about the z-axis passing through the origin, a moire pattern is generated in the lattice structure of bilayer which evolves with twist angle. Based on the twist angle the moire pattern may be commensurate or incommensurate. The work presented here describes the evolution and characteristics of perfectly periodic commensurate moire pattern of TBG.

The commensurate moire pattern is generated through commensurate planar rotation of lattice points of two graphene layers, which obey all rules of planar rotational transformation along with some constraint conditions which allow only those twist angles that generate a perfectly periodic commensurate moire pattern of TBG. To understand the lattice structure of moire pattern in TBG it is sufficient to investigate only planar component (x and y components) of positions of carbon atoms in TBG and the z component can be considered later. Planar positions of coinciding lattice points having triangular lattice symmetry can be arranged on concentric regular hexagons having centre at origin, which have sides of length na_o , (n is a natural number) parallel to vectors $\pm\mathbf{a}_1, \pm\mathbf{a}_2, \pm(\mathbf{a}_1 - \mathbf{a}_2)$ (if the angle between basis vectors is 60°) or parallel to vectors $\pm\mathbf{a}_1, \pm\mathbf{a}_2, \pm(\mathbf{a}_1 + \mathbf{a}_2)$ (if the angle between basis vectors is 120°).

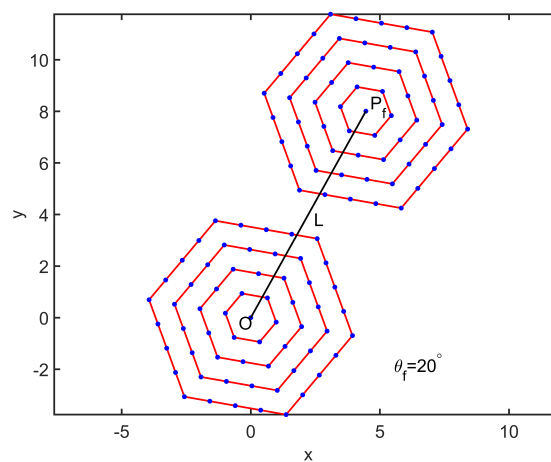
Spacing between any two consecutive hexagons will be $a_o\frac{\sqrt{3}}{2}$. The lattice points lying on a hexagon can be categorized in three categories; corner points, midpoint of sides and points lying between corner and midpoint of sides. The condition for planar rotational transformation is that the initial and final position of point going through



(a)



(b)



(c)

Figure 3: (a) Triangular lattice points arranged on hexagons, Lattice points having same distance from origin, (b) Environment of triangular lattice points in rotated layer around two centres before rotation (c) Environment of triangular lattice points in rotated layer around same two centres after rotation

planar rotational transformation should be at same distance from the origin through which axis of rotation passes. Corresponding to each lattice point, all the lattice points having same distance from origin generally lie on same hexagon but sometimes some of those points might also lie on different hexagons^{3a}. Since whole plane of lattice points is being rotated, therefore the lattice of plane being rotated will remain intact in planar rotational transformation. Since the lattice of plane being rotated remains intact in planar rotational transformation, the environment of lattice points^{3c} around each lattice point in the rotated plane will be same as environment of lattice points around origin even after rotational transformation, although it will be different as compared to environment of lattice points^{3b} before rotation.

The constraint conditions to generate perfectly periodic moire pattern through commensurate planar rotational transformation are determined as follows. Since we are considering origin at the position of a coinciding point, one of the necessary conditions for the generation of a perfectly periodic commensurate moire pattern is that all the superlattice points must be at positions of coinciding lattice points.

Due to three-fold rotational symmetry of graphene plane for the rotation about the normal axis passing through any carbon atom (lattice point), No moire pattern will be generated for twist angles equal to integral multiples of 120° . After a relative twist between the layers through angle equal to 60° , AA-stacked bilayer graphene will be converted into a structure that will have appearance similar to AB stacked bilayer graphene or vice versa, this situation can be considered as the generation of no moire pattern or generation of a moire pattern with infinitely large moire period. Due to six-fold rotational symmetry of plane of coinciding lattice points for the rotation about the normal axis passing through any coinciding lattice points and three fold rotational symmetry of graphene plane, the moire pattern with same characteristics but with changed environment of lattice points around origin and other superlattice points will be generated for twist angles θ , $-\theta$, $60^\circ + \theta$ and $60^\circ - \theta$. The moire patterns generated for twist angles θ , $-\theta$, $60^\circ + \theta$ and $60^\circ - \theta$ will be practically indistinguishable. Therefore, to investigate commensurate moire patterns of twisted bilayer graphene it is sufficient to investigate the commensurate twist angles lying between 0° and 30° .

The moire pattern depends on twist angle of one layer relative to other layer. For simplicity of description, here we consider that the lower layer is static, and the upper layer is rotated about the z axis passing through origin. To investigate the commensurate planar rotational transformation, it is sufficient to investigate only those planar rotational transformations which transfer one coinciding lattice point of upper layer to the position of other coinciding lattice point of same layer, of same type and at same distance from origin.

Since in a perfectly periodic moire pattern the environment of lattice points around each superlattice point must be same therefore it is sufficient to investigate only those

superlattice points which are generated nearest to the origin.

Considering only those superlattice points which are generated nearest to origin; Let there be n such superlattice points and be situated at distance L from origin. These points can be considered to be situated on a circle of radius L and let them be named as $P_{S1}, P_{S2}, P_{S3}, \dots, P_{Sn}$ in a cyclic order. Although in rotated layer the environment of lattice points will be same around each lattice point but in twisted bilayer system the environment of lattice points around each superlattice point might still be different from the environment of lattice points around the origin. The environment of lattice points around each superlattice point would be same if and only if the distance between any two consecutive superlattice points is equal to L , the distance of those superlattice points from origin. $P_{S1}P_{S2} = P_{S2}P_{S3} = \dots = P_{Sn}P_{S1} = L$, such condition can be fulfilled if and only if there are generated only six superlattice points nearest to origin making a regular hexagon of side L , hence generating a perfectly periodic moire pattern with triangular symmetry of superlattice points. The distance L of these superlattice points from origin will be moire period (L_c), the distance between initial and final position of coinciding lattice points which make superlattice points will be minimum commensurate displacement (δ_c) and the twist angle required to generate such moire pattern will be corresponding commensurate twist angle (θ_c). Therefore, for generation of perfectly periodic moire pattern in TBG only those rotational transformations are allowed which generate moire pattern with perfect triangular symmetry of superlattice points around origin and other superlattice points. Therefore, to determine the relationship between commensurate moire period, corresponding minimum commensurate displacement, and corresponding commensurate twist angle of a commensurate moire pattern of TBG, it is sufficient to investigate only those planar rotational transformations which generate a moire pattern in which there are only six superlattice points nearest to origin with triangular symmetry of superlattice points.

If we consider that the superlattice points which are nearest to origin are generated due to rotational transformation of coinciding lattice points of two hexagons then there will be 12 superlattice points nearest to origin, therefore the generated moire pattern will not be perfectly periodic with triangular symmetry of superlattice points. Therefore, we don't need to investigate such rotational transformations of coinciding lattice points of different hexagons. Although a concentric circle can intersect two hexagons in four ways ((1) intersecting sides of inner hexagon and touching the mid points of sides of outer hexagon, (2) intersecting sides of inner hexagon and intersecting sides of outer hexagon, (3) touching the corners of inner hexagon and touching the mid points of sides of outer hexagon, (4) touching the corners of inner hexagon and intersecting sides of outer hexagon) while in FIG.3a only one way is depicted but in all four situations the commensurate rotational transformation between coinciding lattice points of two hexagons will generate 12 superlattice points. Although the rotational transformation of coinciding lattice points of two hexagons can generate valid superlattice points but those superlattice points will not be nearest to origin. Therefore, to determine the rela-

relationship between commensurate moire period, corresponding minimum commensurate displacement, and corresponding commensurate twist angle of a commensurate moire pattern of TBG, it is sufficient to investigate only those rotational transformations which occur among coinciding lattice points lying on same hexagon.

Six corners of a hexagon have same distance from the origin, if we consider rotational transformation of lattice point from one corner of a hexagon to other corner of the same hexagon, this type of rotational transformation will take place for twist angles equal to integral multiples of 60° , which will not produce moire pattern. Six midpoints of sides of a hexagon have same distance from the origin, if we consider the rotational transformation of lattice point from mid-point of one side of a hexagon to mid-point of other side of the same hexagon, this type of rotational transformation will take place for twist angles equal to integral multiples of 60° , which will not produce moire pattern.

Only possibility remaining to investigate is the generation of commensurate superlattice points, which lie nearest to origin, by rotational transformation among coinciding lattice points which lie between corners and midpoint of sides of same hexagon and have same distance from origin. Each side of hexagon contains two such coinciding lattice points which have same distance from origin. Consider the coinciding lattice points lying on a hexagon of side length equal to na_o . Let us denote its corners by C_1, C_2, \dots, C_6 and the mid points of side by M_1, M_2, \dots, M_6 . Between a corner and mid-point of a side of this hexagon there will be $(p - 1)$ coinciding lattice points where $p = \left(\frac{n+rem(n,2)}{2}\right)$ and $rem(n, 2) = 0$ if n is even or $rem(n, 2) = 1$ if n is odd. Let us assign an index $k = 1, 2, \dots, (p - 1)$ to these points. The distance of k^{th} coinciding lattice point from mid-point of its parent side will be equal to $ka_o - rem(n, 2)\frac{a_o}{2}$. The distance of this k^{th} coinciding lattice point from origin will be equal to

$$L_{n,k} = \sqrt{\left(na_o\frac{\sqrt{3}}{2}\right)^2 + \left(ka_o - rem(n, 2)\frac{a_o}{2}\right)^2} = \frac{a_o}{2}\sqrt{3n^2 + (2k - rem(n, 2))^2}.$$

Corresponding to each index k there will be 12 coinciding lattice points of same type on a hexagon denoted by $P_{1,n,k}, P_{2,n,k}, \dots, P_{12,n,k}$ which will have same distance from origin (as shown in FIG. 4, n, k part of index is omitted). The distance between any two consecutive points taken in cyclic order will be equal to $\delta_{1,n,k} = (2k - rem(n, 2))a_o$ if they are situated on same side of hexagon or equal to $\delta_{2,n,k} = \sqrt{3}(n - 2k + rem(n, 2))a_o$ if they are situated on adjacent sides of hexagon. The distance between alternate points will be equal to $L_{n,k}$, distance of these points from origin, thus making 60° angle at origin.

To investigate twist angles lying between 0° and 30° , it is sufficient to investigate the planar rotational transformation among any 3 consecutive coinciding lattice points. Let us consider rotational transformation among 3 consecutive coinciding lattice points $P_{1,n,k}, P_{2,n,k}, P_{3,n,k}$. For rotational transformation among these three coinciding lattice points there can be three commensurate displacements $P_{1,n,k}P_{2,n,k} = \delta_{1,n,k}$, $P_{2,n,k}P_{3,n,k} = \delta_{2,n,k}$ and $P_{1,n,k}P_{3,n,k} = L_{n,k}$. The rotational transformation correspond-

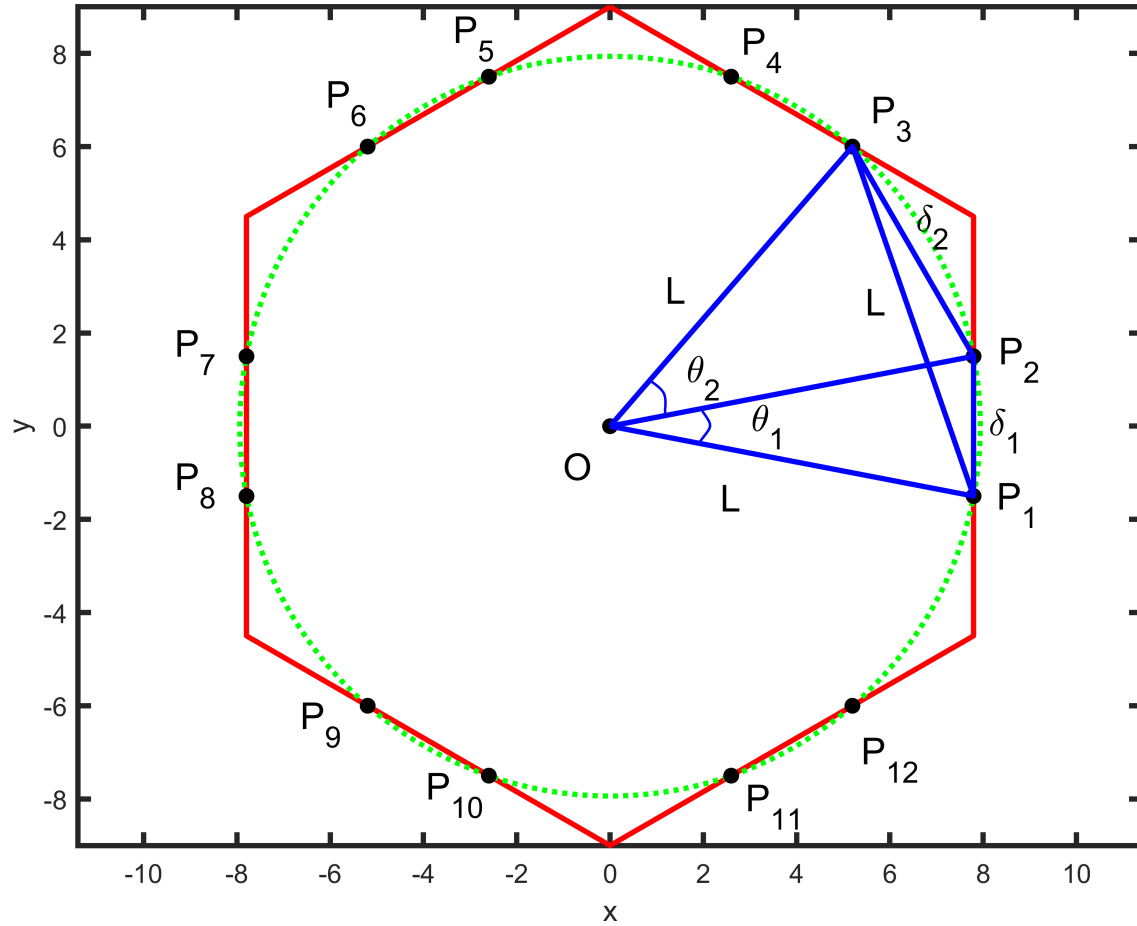


Figure 4: Commensurate rotation between coinciding lattice points of same hexagon

ing to commensurate displacement $P_{1,n,k}P_{3,n,k} = L_{n,k}$ will occur for twist angle equal to 60° , hence no moire pattern will be generated. The rotational transformation corresponding to commensurate displacement $P_{1,n,k}P_{2,n,k} = \delta_{1,n,k}$ will occur for twist angle equal to $\theta_{1,n,k} = 2 \sin^{-1} \left(\frac{\delta_{1,n,k}}{2L_{n,k}} \right)$ and the rotational transformation corresponding to commensurate displacement $P_{2,n,k}P_{3,n,k} = \delta_{2,n,k}$ will occur for twist angle equal to $\theta_{2,n,k} = 2 \sin^{-1} \left(\frac{\delta_{2,n,k}}{2L_{n,k}} \right)$. It is worth noting that $\theta_{1,n,k} + \theta_{2,n,k} = 60^\circ$, Therefore, moire pattern with same characteristics will be generated for twist angles $\theta_{1,n,k}$ and $\theta_{2,n,k}$. Therefore, corresponding to commensurate moire period $L_{n,k}$ we associate either $\theta_{1,n,k}$ or $\theta_{2,n,k}$ as θ_c , whichever is smaller than 30° also the corresponding commensurate displacement δ_c is chosen accordingly.

Every Commensurate rotation will generate infinite number of superlattice points at different distances from origin, which will have correspondingly different values of commensurate displacement between initial and final position of corresponding coinciding lattice point but the ratio of corresponding commensurate displacement to distance

of superlattice point from origin will be same for all those superlattice points. Same value of θ_c will come from all those pairs (n, k) which have same ratio of corresponding commensurate displacement to distance of superlattice point from origin. Therefore, while choosing moire period (L_c) and minimum commensurate displacement (δ_c) for any commensurate twist angle θ_c we choose that pair of (n, k) , which have lowest value of $L_{n,k}$ i.e., which corresponds to superlattice points which are generated nearest to origin.

Table 1: A short list of moire period (L_c in units of a_o), corresponding minimum commensurate displacement (δ_c in units of a_o) and commensurate twist angle (θ_c in degree) in commensurate TBG

L_c	δ_c	θ_c
90.0722	2	1.2722
78.5048	1.7320	1.2641
45.9021	1	1.2482
80.5046	1.7320	1.2327
93.5361	2	1.2251
81.5046	1.7320	1.2176
47.6340	1	1.2028
83.5045	1.7320	1.1884
97	2	1.1814
84.5044	1.7320	1.1744
49.3660	1	1.1606
86.5043	1.7320	1.1472
87.5043	1.7320	1.1341
51.0979	1	1.1213
89.5042	1.7320	1.1088
90.5041	1.7320	1.0965
52.8299	1	1.0845
92.5040	1.7320	1.0728
93.5040	1.7320	1.0614
54.5619	1	1.0501
95.5039	1.7320	1.0391
96.5038	1.7320	1.0284
56.2939	1	1.0178
98.5038	1.7320	1.0075
99.5038	1.7320	0.9974
58.0258	1	0.9874

Using this description of commensurate moire pattern in TBG a computational code

is written in MATLAB to generate a list of commensurate twist angle and minimum commensurate displacement corresponding to commensurate moire period lying between a_o and $100a_o$ (this range can be further increased). The list contains around 1400 commensurate twist angles lying in range $0^\circ - 30^\circ$. A part of that list is shown in TABLE 1. If we increase the limit of moire period in the code from $100a_o$ to even larger value, then many more commensurate twist angles (lying in range $0^\circ - 30^\circ$) appear in the generated list and the difference between any two consecutive commensurate twist angles decreases. If we keep increasing the limit of moire period in the code then the difference between any two consecutive commensurate twist angles keep decreasing.

3. Apparent strain and rotational symmetry breaking in moire pattern of commensurate TBG

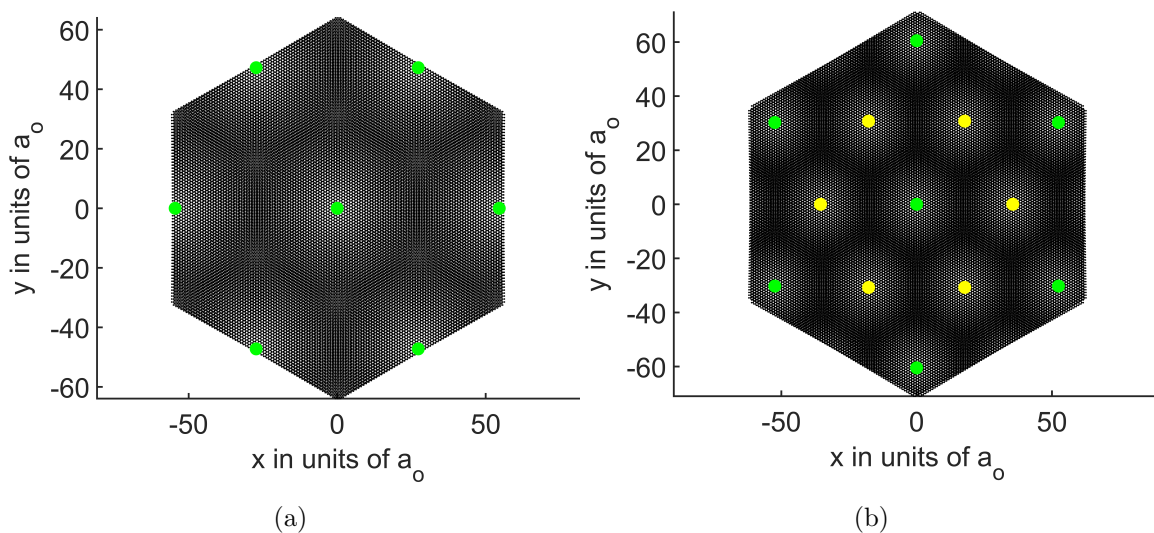


Figure 5: (a) Simulated moire pattern of TBG for $\theta_c = 1.05^\circ$, $L_c = 54.562a_o$ and $\delta_c = 1a_o$ (b) Simulated moire pattern of TBG for $\theta_c = 1.64^\circ$, $L_c = 60.506a_o$ and $\delta_c = \sqrt{3}a_o$, green points are actual superlattice points and yellow points are apparent superlattice points other than actual superlattice points

For further investigation of commensurate moire pattern in TBG, computational codes are made to simulate planar position of carbon atoms in a crystal of TBG which is generated after introducing relative twist between two graphene layers of hexagonal crystal of conventional bilayer graphene which has side length equal to $\frac{2}{\sqrt{3}}L_c$. Length of side of hexagonal crystal of bilayer graphene is chosen to be $\frac{2}{\sqrt{3}}L_c$, so that it can at least accommodate six superlattice points lying nearest to origin. We tried to simulate moire patterns of TBG for many commensurate twist angles near magic angle and the generated moire patterns appear to have triangular symmetry of superlattice points. It is surprising to encounter that for commensurate twist angles which are associated with

value of minimum commensurate displacement (δ_c) other than a_o , the moire period of moire pattern 5b appears quite different from actual moire period (L_c), let such moire patterns be named as anomalous commensurate moire patterns. For commensurate twist angles which are associated with value of minimum commensurate displacement (δ_c) equal to a_o , the moire period of moire pattern 5a appears to be same as actual moire period (L_c), let such moire patterns be named as normal commensurate moire patterns.

To investigate the generated moire patterns thoroughly we decided to find the value of moire period in generated moire patterns of TBG. To find the value of moire period in generated moire pattern we tried to find the locations of actual superlattice points via finding positions of perfectly coinciding sublattice points of same type which coincide on origin in moire pattern. If we consider AA-stacked bilayer before rotation, then we consider origin on a site where A_1 and A_2 sublattices coincide and if we consider AB-stacked bilayer before rotation, then we consider origin on a site where A_1 and B_2 sublattices coincide. If we consider AA-stacked bilayer before rotation, then actual superlattice points will be located where the planar distance between A_1 and A_2 sublattice points of two layers become exactly zero and if we consider AB-stacked bilayer before rotation then, actual superlattice points will be located where the planar distance between A_1 and B_2 sublattice points of two layers become exactly zero. We considered AA-stacked bilayer before rotation and origin at a site where A_1 and A_2 sublattices coincide. To find the positions of actual superlattice points in TBG the planar distances between A_1 and A_2 sublattice points of two layers are computed and the positions of actual superlattice points are found. In normal moire patterns the positions of actual superlattice points (depicted by green dots 5a) are found to be situated in the centre of each AA-type looking regions of moire pattern. Using the positions of actual superlattice points, distances between actual superlattice points are computed and the distance between any two actual superlattice points which are nearest to each other is found to be exactly same as L_c . Therefore, normal commensurate moire patterns have perfect triangular symmetry of superlattice points and there is no intrinsic strain in normal commensurate moire patterns of TBG.

In anomalous commensurate moire patterns actual superlattice points (depicted by green dots 5b) occupy centre of not all but only some of the AA-type looking regions of moire pattern. Using the positions of actual superlattice points, distances between actual superlattice points are computed and the distance between any two actual superlattice points which are nearest to each other is found to be exactly same as L_c . But what about remaining AA-type looking regions, they also seem similar to other AA-type looking regions occupied with actual superlattice points. To investigate deeply we tried to locate the points where the planar distance between A_1 and A_2 sublattice points of two layers is very close to zero but not exactly zero. Depending on the upper limit of that very small positive number being used for comparison of planar distance between A_1 and A_2 sublattice points of two layers, every AA-type looking region of anomalous moire patterns is found to contain few such points where

Twist Angle, Strain, Broken Rotational Symmetry, Corrugation and Supercell in TBG14

Table 2: A short list of moire period (L_c in units of a_o), corresponding minimum commensurate displacement δ_c (in units of a_o), twist angle θ_c (in degree), average value of apparent moire period ($Avg.L_{app}$ in units of a_o), maximum value of apparent moire period ($Max.L_{app}$ in units of a_o), minimum value of apparent moire period ($Min.L_{app}$ in units of a_o) and apparent strain in moire pattern (in %) of commensurate TBG

L_c	δ_c	θ_c	$Avg.L_{app}$	$Max.L_{app}$	$Min.L_{app}$	Strain
90.0722	2	1.2722	45.0361	45.9021	44.1701	3.8457
78.5048	1.7320	1.2641	45.3248	45.9021	45.0333	1.9167
45.9021	1	1.2482	45.9021	45.9021	45.9021	0.0
80.5046	1.7320	1.2327	46.4794	47.6340	45.9021	3.7263
93.5361	2	1.2251	46.7680	47.6340	45.9021	3.7033
81.5046	1.7320	1.2176	47.0567	47.6340	46.7654	1.8460
47.6340	1	1.2028	47.6340	47.6340	47.6340	0.0
83.5045	1.7320	1.1884	48.2113	48.5077	47.6340	1.8122
97	2	1.1814	48.5	49.3660	47.6340	3.5710
84.5044	1.7320	1.1744	48.7887	49.3660	48.4974	1.7802
49.3660	1	1.1606	49.3660	49.3660	49.3660	0.0
86.5043	1.7320	1.1472	49.9433	51.0979	49.3660	3.4679
87.5043	1.7320	1.1341	50.5206	51.0979	50.2295	1.7190
51.0979	1	1.1213	51.0979	51.0979	51.0979	0.0
89.5042	1.7320	1.1088	51.6753	51.9711	51.0979	1.6898
90.5041	1.7320	1.0965	52.2526	52.8299	51.9615	1.6619
52.8299	1	1.0845	52.8299	52.8299	52.8299	0.0
92.5040	1.7320	1.0728	53.4072	54.5619	52.8299	3.2430
93.5040	1.7320	1.0614	53.9846	54.5619	53.6936	1.6085
54.5619	1	1.0501	54.5619	54.5619	54.5619	0.0
95.5039	1.7320	1.0391	55.1392	55.4346	54.5619	1.5828
96.5039	1.7320	1.0284	55.7165	56.2939	54.5619	3.1086
56.2939	1	1.0178	56.2939	56.2939	56.2939	0.0
98.5038	1.7320	1.0075	56.8712	58.0259	56.2939	3.0455
99.5038	1.7320	0.9974	57.4485	58.0259	57.1577	1.5112
58.0258	1	0.9874	58.0258	58.0258	58.0258	0.0

the planar distance between A_1 and A_2 sublattice points of two layers is very close to zero but not exactly zero. For every AA-type looking region of anomalous moire patterns we choose only one out of those points which has minimum value of the planar distance between A_1 and A_2 sublattice points of two layers, let such points (other than actual superlattice points) be named as apparent superlattice points (depicted by yellow dots5b). Using the positions of apparent superlattice points and actual superlattice points the value of apparent moire period is determined. For anomalous moire patterns we get multiple slightly different values of apparent moire period and the average value of apparent moire period $Avg.L_{app}$ comes to be approximately equal to L_c/δ_c . From these multiple slightly different values of apparent moire period, maximum ($Max.L_{app}$) and minimum ($Min.L_{app}$) value of apparent moire period are determined. Therefore, actual superlattice points of anomalous moire patterns form a triangular lattice of lattice constant exactly equal to L_c and neither there is intrinsic strain nor intrinsic rotational symmetry breaking. But apparent superlattice points along with actual superlattice points of anomalous moire patterns form a triangular lattice of lattice constant approximately equal to L_c/δ_c and it appears that there is intrinsic strain and intrinsic rotational symmetry breaking in anomalous moire patterns. Presence of similar looking apparent superlattice points along with actual superlattice points causes intrinsic strain and intrinsic rotational symmetry breaking to appear in anomalous moire patterns of TBG. Therefore, experimentally observed strain and rotational symmetry breaking in moire patterns of TBG may be due to misunderstanding apparent superlattice points as actual superlattice points. The apparent strain in anomalous moire pattern of TBG is calculated using following formula:

$$(\text{Strain in } \%) = 100 \left(\frac{Max.L_{app} - Min.L_{app}}{Avg.L_{app}} \right).$$

TABLE 2 present a small list of computed apparent strain in moire pattern of commensurate TBG for some commensurate twist angles near magic angle.

4. corrugation in TBG

Unlike conventional bilayer graphene, interlayer distance in TBG is not uniform rather TBG has corrugated structure[5, 20, 24] which appears as there are 2-dimensional cosine like peaks (crests) at centre of each AA-type looking region which die to minimum (troughs) at centre of AB-type looking region. This variation of interlayer distance in TBG is called as corrugation in TBG. Evolution of corrugation in TBG can be described as follows. In AA-stacked bilayer graphene the interlayer distance is maximum ($d_{\perp AA} = 3.55\text{\AA}$) but it is least stable bilayer structure of graphene on the other hand in AB-stacked bilayer graphene the interlayer distance is minimum ($d_{\perp AB} = 3.35\text{\AA}$) and it is most stable bilayer structure of graphene. In AA-stacked bilayer graphene all the p_z orbitals and all C-C bonds of two graphene layers are perfectly aligned. In AB-stacked bilayer graphene only half of the p_z orbitals of two graphene layers are aligned and all C-C bonds of two graphene layers are most mis-aligned among all bilayer graphene structures. Two graphene layers of AB-stacked bilayer graphene are attracted towards each other

by a force which holds them together, but this attractive force is so weak that graphene layers can slide on one another easily. From these observations we can infer that partial overlap of p_z orbitals of two graphene layers causes attraction between the graphene layers and repulsion between electron pairs of C-C bonds of two graphene layers causes repulsion between two graphene layers. In AA-stacked bilayer graphene the repulsion between two graphene layers is maximum, therefore, AA-stacked bilayer graphene is least stable bilayer graphene and interlayer distance in AA-stacked bilayer graphene is maximum among all bilayer graphene structures. In AB-stacked bilayer graphene the repulsion between two graphene layers is minimum, therefore, AB-stacked bilayer graphene is most stable bilayer graphene and interlayer distance in AB-stacked bilayer graphene is minimum among all bilayer graphene structures. In TBG environment of p_z orbitals and C-C bonds is different around each carbon atom in a supercell and similar supercells occur periodically. In a supercell of TBG the alignment of C-C bonds of two graphene layers varies from most aligned (in comparison to other regions of same TBG) at the centre of AA-type looking region to least aligned (in comparison to other regions of same TBG) at the centre of AB-type looking region. Therefore, in a supercell of TBG the repulsion between two graphene layers smoothly varies from maximum (in comparison to other regions of same TBG) at the centre of AA-type looking region to minimum (in comparison to other regions of same TBG) at the centre of AB-type looking region. This periodically and smoothly varying repulsion between two graphene layers in TBG produces periodically and smoothly varying interlayer distance or corrugation in TBG which have maximum interlayer distance ($Max.d_{\perp TBG}$) at centre of AA-type looking region and minimum interlayer distance ($Min.d_{\perp TBG}$) at centre of AB-type looking region. Corrugation in TBG would induce strain in sigma bonds of graphene network. Since the corrugation is caused by weak repulsion between graphene layers which is very weak in comparison to strong C-C sigma bonds, therefore, the magnitude of corrugation ($\Delta d_{\perp TBG}$), which is defined as half of the difference between maximum and minimum interlayer distance in TBG, would be such that the strain in sigma bonds network of graphene caused by the corrugation in TBG would be very small also to minimize the strain in sigma bonds network of graphene in TBG, height of carbon atoms in graphene plane in TBG should vary very slowly and smoothly. TBG corresponding to twist angle 0° can be considered as a TBG system consisted of infinitely large AA-stacked bilayer graphene combined with infinitely large AB-stacked bilayer graphene. The junction of two regions would not be sharp but it will be slowly and smoothly varying transition from one type of region to other type of region, also the span of junction region would be infinitely large. Interlayer distance of TBG is maximum at the centre of AA-type looking region and minimum at the centre of AB-type looking region. In TBG corresponding to twist angle 0° the magnitude of corrugation is maximum, but the interlayer distance changes slowly and smoothly over infinitely large span, therefore, the strain in sigma bonds network of graphene in such TBG would be almost zero. As the twist angle increases from 0° , C-C bonds of two layers move towards more aligned structure in AB-type looking region and C-C bonds of two layers move towards less aligned structure in

AA-type looking region, therefore, the repulsion between two graphene layers decreases in AA-type looking region while the repulsion between two layers increases in AB-type looking region. Therefore, as the twist angle increases maximum interlayer distance of TBG decreases and minimum interlayer distance of TBG increases. Since the moire pattern corresponding to twist angle θ and $60^\circ - \theta$ are practically same, therefore, as the twist angle increases, maximum interlayer distance of TBG decreases and minimum interlayer distance of TBG increases till the twist angle of 30° is reached and after the twist angle of 30° the trend of maximum and minimum interlayer distance is reversed symmetrically. To minimize strain in sigma bonds network of graphene in TBG, the magnitude of corrugation would be very small as compared to apparent moire period and it would vary as slow or fast with twist angle as the apparent moire period does. For twist angles which are very close to 0° , the apparent moire period will be so large that even with maximum magnitude of corrugation, the strain induced in sigma bonds network of graphene in TBG would be practically almost zero. Therefore, for twist angles which are very close to 0° , the magnitude of corrugation would decrease so slowly that practically it would be same as maximum value of magnitude of corrugation. This type of behaviour of interlayer distance in TBG can be represented mathematically by following formulation:

$$Avg.L_{app} = L_c/\delta_c = \frac{1}{2 \sin\left(\frac{\theta_c}{2}\right)} \quad (1)$$

$$\Delta d_{\perp TBG} = \frac{\begin{pmatrix} \alpha_{11} (d_{\perp AA} - d_{\perp AB}) \exp(-\alpha_{12} |\sin(3\theta_C)|^{\alpha_{13}}) \\ +\alpha_{21} (d_{\perp AA} - d_{\perp AB}) \exp(-\alpha_{22} |\sin(3\theta_C)|^{\alpha_{23}}) \\ +\alpha_{31} (d_{\perp AA} - d_{\perp AB}) \exp(-\alpha_{32} |\sin(3\theta_C)|^{\alpha_{33}}) \\ +0.001 (\alpha_{11} + \alpha_{21} + \alpha_{31}) (d_{\perp AA} - d_{\perp AB}) (1 - \exp(-|\sin(3\theta_C)|)) \end{pmatrix}}{2(\alpha_{11} + \alpha_{21} + \alpha_{31})} \quad (2)$$

$$Avg.d_{\perp TBG} = 0.5(d_{\perp AA} + d_{\perp AB}) \quad (3)$$

$$Max.d_{\perp TBG} = Avg.d_{\perp TBG} + \Delta d_{\perp TBG} \quad (4)$$

$$Min.d_{\perp TBG} = Avg.d_{\perp TBG} - \Delta d_{\perp TBG} \quad (5)$$

Average value of apparent moire period is given by equation 1 and its variation with twist angle in TBG is shown in figure6a. Magnitude of corrugation is given by equation 2. Variation of magnitude of corrugation with twist angle in TBG is shown in figure 6b. Values of parameters used in equation2 are $\alpha_{11} = 10$, $\alpha_{12} = 200$, $\alpha_{13} = 1.9$, $\alpha_{21} = 7$, $\alpha_{22} = 30$, $\alpha_{23} = 1.9$, $\alpha_{31} = 3$, $\alpha_{32} = 3$, $\alpha_{33} = 1.9$, which are estimated by attempting to achieve same type of variation of apparent moire period and magnitude of corrugation. Average interlayer distance ($Avg.d_{\perp TBG}$) is given by equation3, it is same for all twist angles in TBG and its variation with twist angle in TBG is shown in figure 6c. Maximum ($Max.d_{\perp TBG}$) and minimum ($Min.d_{\perp TBG}$) interlayer distance in TBG are given by equation4 and equation5 respectively and their variation with twist angle in TBG is shown in figure 6d.

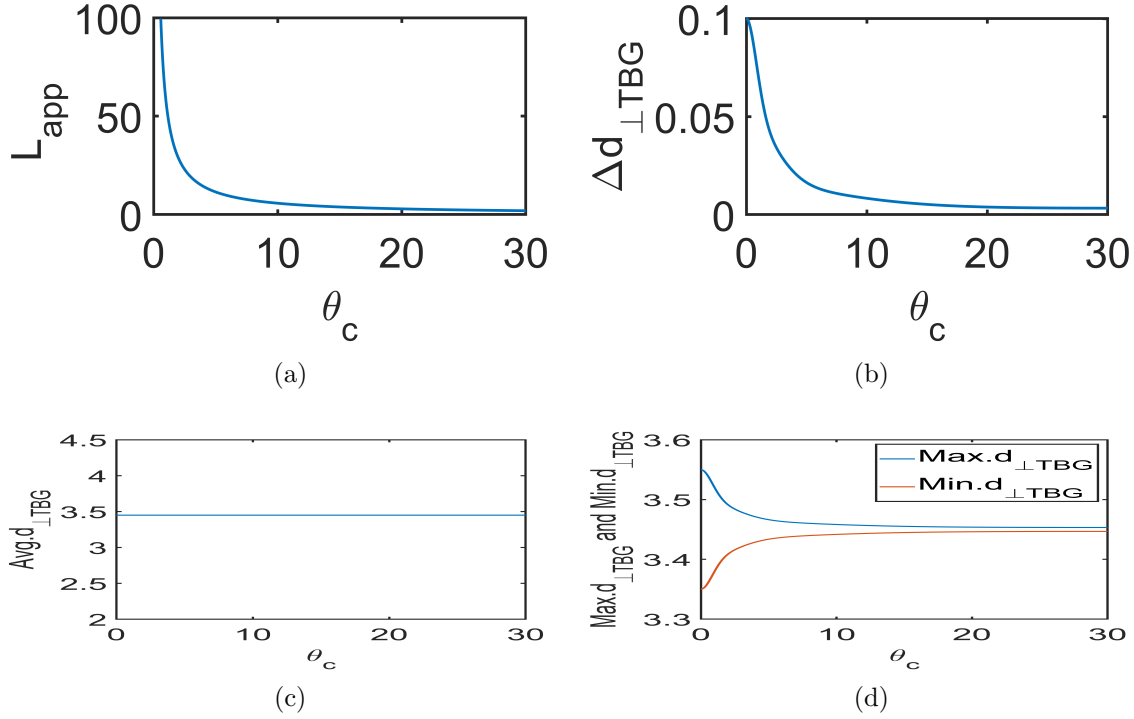


Figure 6: (a) Variation of apparent moire period (in units of a_o) with twist angle (in degree) in TBG (b) Variation of magnitude of corrugation (in units of \AA) with twist angle (in degree) in TBG, (c) variation of average interlayer distance (in units of \AA) with twist angle (in degree) in TBG (d) Variation of maximum and minimum interlayer distance (in units of \AA) with twist angle (in degree) in TBG

After determining the magnitude of corrugation in TBG, z-coordinates of carbon atoms in two graphene layers of TBG are determined on the basis of their distance from the centre of nearest AA-type looking region. z-coordinates of carbon atoms in two graphene layers of TBG are given by equations 6a, 6b, 6c, 6d.

$$Z_{A_1(m)} = -0.5 \left(\text{Min}.d_{\perp TBG} + (\text{Max}.d_{\perp TBG} - \text{Min}.d_{\perp TBG}) \left(\cos \left(\frac{\pi}{2a} \left(r_{A_1(m), \text{nearest } A_2}^{\parallel} \right) \right) \right)^{\alpha_o} \right) \quad (6a)$$

$$Z_{B_1(m)} = -0.5 \left(\text{Min}.d_{\perp TBG} + (\text{Max}.d_{\perp TBG} - \text{Min}.d_{\perp TBG}) \left(\cos \left(\frac{\pi}{2a} \left(r_{B_1(m), \text{nearest } B_2}^{\parallel} \right) \right) \right)^{\alpha_o} \right) \quad (6b)$$

$$Z_{A_2(m)} = 0.5 \left(\text{Min}.d_{\perp TBG} + (\text{Max}.d_{\perp TBG} - \text{Min}.d_{\perp TBG}) \left(\cos \left(\frac{\pi}{2a} \left(r_{A_2(m), \text{nearest } A_1}^{\parallel} \right) \right) \right)^{\alpha_o} \right) \quad (6c)$$

$$Z_{B_2(m)} = 0.5 \left(\text{Min}.d_{\perp TBG} + (\text{Max}.d_{\perp TBG} - \text{Min}.d_{\perp TBG}) \left(\cos \left(\frac{\pi}{2a} \left(r_{B_2(m), \text{nearest } B_1}^{\parallel} \right) \right) \right)^{\alpha_o} \right) \quad (6d)$$

$Z_{A_1(m)}$ is z-coordinate of carbon atom situated at m^{th} lattice point of A_1 sublattice, $Z_{B_1(m)}$ is z-coordinate of carbon atom situated at m^{th} lattice point of B_1 sublattice, $Z_{A_2(m)}$ is z-coordinate of carbon atom situated at m^{th} lattice point of A_2 sublattice and $Z_{B_2(m)}$ is z-coordinate of carbon atom situated at m^{th} lattice point of B_2 sublattice. $r_{A_1(m), \text{nearest } A_2}^{\parallel}$ is planar distance (in units of a) of carbon atom situated at m^{th} lattice

point of A_1 sublattice from nearest carbon atom of A_2 sublattice. $r_{B_1(m),nearest B_2}^{\parallel}$ is planar distance (in units of a) of carbon atom situated at m^{th} lattice point of B_1 sublattice from nearest carbon atom of B_2 sublattice. $r_{A_2(m),nearest A_1}^{\parallel}$ is planar distance (in units of a) of carbon atom situated at m^{th} lattice point of A_2 sublattice from nearest carbon atom of A_1 sublattice. $r_{B_2(m),nearest B_1}^{\parallel}$ is planar distance (in units of a) of carbon atom situated at m^{th} lattice point of B_2 sublattice from nearest carbon atom of B_1 sublattice. $\alpha_o = 3.0$ is a parameter to control smoothness of corrugation in TBG.

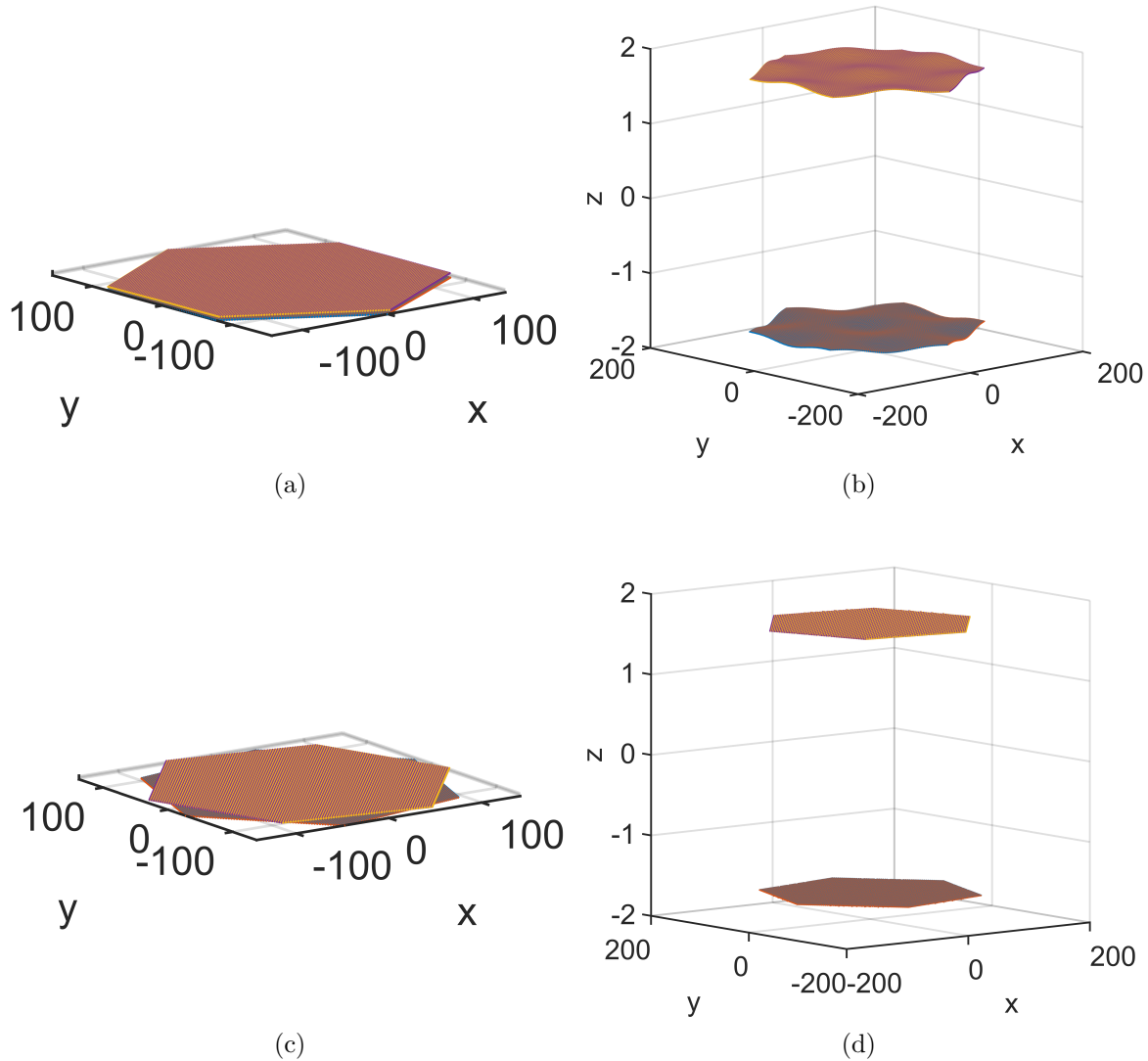


Figure 7: (a),(b) Corrugation in TBG with twist angle 1.0501° (c), (d) Corrugation in TBG with twist angle 29.9886°

We modified the computational code which was written to simulate planar position of carbon atoms by incorporating z-coordinate of carbon atoms along with planar positions. Both figure7a and figure7b show corrugation in structure of TBG with twist angle equal to 1.0501° . Both figure7c and figure7d show corrugation in structure of

TBG with twist angle equal to 29.9886° . In figure 7a and 7c the scale of all axes is same, and it seems that both graphene layers are flat, which indicate that magnitude of corrugation is very small in comparison to period of moire pattern. In figure 7b and 7d the scale of planar axes is converged, and scale of z-axis is diverged to visualise corrugation in TBG. In TBG with twist angle equal to 1.0501° , magnitude of corrugation is 0.0683\AA , maximum interlayer distance is (3.5183\AA) and minimum interlayer distance is (3.3817\AA) . In TBG with twist angle equal to 29.9986° magnitude of corrugation is 0.0008\AA , which is very small. Due to very small value of magnitude of corrugation the maximum interlayer distance (3.4508\AA) , minimum interlayer distance (3.4492\AA) and average interlayer distance (3.45\AA) are almost same[25].

5. Internal configuration of carbon atoms inside the supercell of TBG

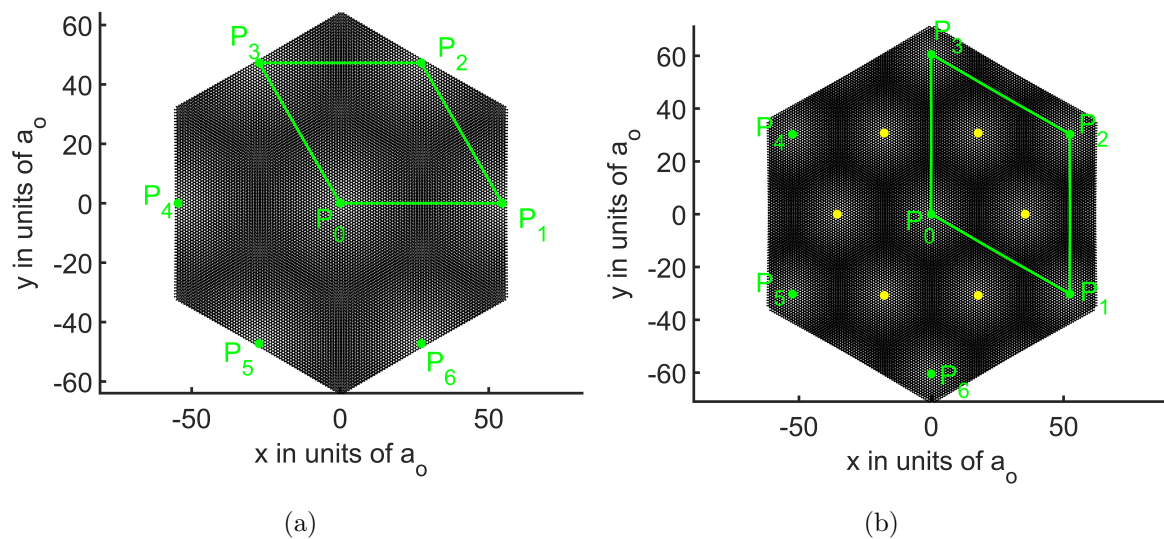


Figure 8: (a) Supercell of moire pattern in TBG with twist angle equal to 1.0501° and corresponding minimum commensurate displacement $\delta_c = a_o$ (b) Supercell of moire pattern in TBG with twist angle equal to 1.6402° and corresponding minimum commensurate displacement $\delta_c = \sqrt{3}a_o$

While simulating moire pattern in TBG for various commensurate twist angles we observe a pattern in positions of actual superlattice points. If we introduce relative twist between two graphene layers by angle θ_c in such a way that the lower layer is twisted by angle $\theta_1 = -0.5\theta_c$ (in clockwise direction) and upper layer is twisted by angle $\theta_2 = +0.5\theta_c$ (in anticlockwise direction), then the actual superlattice points which are nearest to origin will be situated at distance L_c from origin and their positions will be in directions of midpoint of sides or in directions of corners of regular hexagons which have sides parallel to vectors $\pm\mathbf{a}_1, \pm\mathbf{a}_2, \pm(\mathbf{a}_1 - \mathbf{a}_2)$ (if the angle between basis vectors is 60°) or parallel to vectors $\pm\mathbf{a}_1, \pm\mathbf{a}_2, \pm(\mathbf{a}_1 + \mathbf{a}_2)$ (if the angle between basis vectors

is 120°) and centre at origin (recall figure 3a,4).

If the minimum commensurate displacement δ_c corresponding to twist angle θ_c is integral multiple of a_o then the positions of actual superlattice points will be in directions of midpoint of sides of hexagons shown in figure3a. If the minimum commensurate displacement δ_c corresponding to twist angle θ_c is integral multiple of $\sqrt{3}a_o$ then the positions of actual superlattice points will be in directions of corners of hexagons shown in figure3a. Therefore, if the minimum commensurate displacement δ_c corresponding to twist angle θ_c is integral multiple of a_o then the positions of actual superlattice points, as shown in figure 8a, which are nearest to origin ($P_0 \equiv (0.0, 0.0)$, 0 is index for actual superlattice point at origin) will be $P_1 \equiv (L_c, 0.0)$, $P_2 \equiv \left(\frac{L_c}{2}, \frac{\sqrt{3}L_c}{2}\right)$, $P_3 \equiv \left(-\frac{L_c}{2}, \frac{\sqrt{3}L_c}{2}\right)$, $P_4 \equiv (-L_c, 0.0)$, $P_5 \equiv \left(-\frac{L_c}{2}, -\frac{\sqrt{3}L_c}{2}\right)$, $P_6 \equiv \left(\frac{L_c}{2}, -\frac{\sqrt{3}L_c}{2}\right)$. If the minimum commensurate displacement δ_c corresponding to twist angle θ_c is integral multiple of $\sqrt{3}a_o$ then the positions of actual superlattice points, as shown in figure 8b, which are nearest to origin will be $P_1 \equiv \left(\frac{\sqrt{3}L_c}{2}, -\frac{L_c}{2}\right)$, $P_2 \equiv \left(\frac{\sqrt{3}L_c}{2}, \frac{L_c}{2}\right)$, $P_3 \equiv (0, L_c)$, $P_4 \equiv \left(-\frac{\sqrt{3}L_c}{2}, \frac{L_c}{2}\right)$, $P_5 \equiv \left(-\frac{\sqrt{3}L_c}{2}, -\frac{L_c}{2}\right)$, $P_6 \equiv (0, -L_c)$. Region enclosed by parallelogram $P_0P_1P_2P_3$ can be considered as supercell of TBG (shown in figure 8a 8b). Recall that computational code can be used to simulate planar position of carbon atoms in a crystal of TBG which is generated after introducing relative twist between two graphene layers of hexagonal crystal of conventional bilayer graphene which has side length equal to $\frac{2}{\sqrt{3}}L_c$. Let us name the set of positions of carbon atoms constituting this crystal as set S_1 . Position of atoms lying inside the supercell of TBG can be extracted from set S_1 by using concept of polar angle and some other basic concepts of geometry. In polar coordinate system polar angle is given by $\varphi = \cos^{-1} \frac{x}{\sqrt{x^2+y^2}}$ if $y \geq 0$ and $\sqrt{x^2+y^2} \neq 0$ or $\varphi = -\cos^{-1} \frac{x}{\sqrt{x^2+y^2}}$ if $y < 0$ or $\varphi = \text{undefined}$ if $\sqrt{x^2+y^2} = 0$. φ lies in range $(-180^\circ, 180^\circ]$.

Case:(1) If the minimum commensurate displacement δ_c corresponding to twist angle θ_c is integral multiple of a_o : the value polar angle for positions of carbon atoms lying inside the supercell will lie in range $[0^\circ, 120^\circ]$. Let us define a set S_2 which is a subset of S_1 . S_2 contains only those elements of S_1 which have corresponding value of polar angle lying in range $[0^\circ, 120^\circ]$. x-coordinate of lattice points of supercell will lie in range $[-0.5L_c, L_c)$ and y-coordinate of lattice points will lie in range $\left[0, L_c \frac{\sqrt{3}}{2}\right)$. We define S_3 as a subset of S_2 which contains only those elements of S_2 that satisfy condition; x-coordinate of lattice point is in range $\left(\frac{1}{2}L_c, L_c\right)$ and y-coordinate of lattice point is in range $[0, \sqrt{3}(L_c - x))$. We define S_4 as a subset of S_2 which contains only those elements of S_2 that satisfy condition; x-coordinate of lattice point is in range $\left[-\frac{1}{2}L_c, \frac{1}{2}L_c\right]$ and y-coordinate of lattice point is in range $\left[0, \frac{\sqrt{3}}{2}L_c\right)$. Supercell will be union of S_3 and S_4 .

Case:(2) If the minimum commensurate displacement δ_c corresponding to twist angle θ_c is integral multiple of $\sqrt{3}a_o$: the value polar angle for positions of carbon atoms lying inside the supercell will lie in range $[-30^\circ, 90^\circ]$. Let us define a set S_2 which is a subset of

S_1 . S_2 contains only those elements of S_1 which have corresponding value of polar angle lying in range $[-30^\circ, 90^\circ]$. x-coordinate of lattice points of supercell will lie in range $\left[0, \frac{\sqrt{3}}{2}L_c\right)$ and y-coordinate of lattice points will lie in range $\left[-\frac{x}{\sqrt{3}}, L_c - \frac{x}{\sqrt{3}}\right)$. Supercell will be a subset of S_2 which contains only those elements of S_2 that satisfy condition; x-coordinate of lattice points is in range $\left[0, \frac{\sqrt{3}}{2}L_c\right)$ and corresponding y-coordinate of lattice points is in range $\left[-\frac{x}{\sqrt{3}}, L_c - \frac{x}{\sqrt{3}}\right)$.

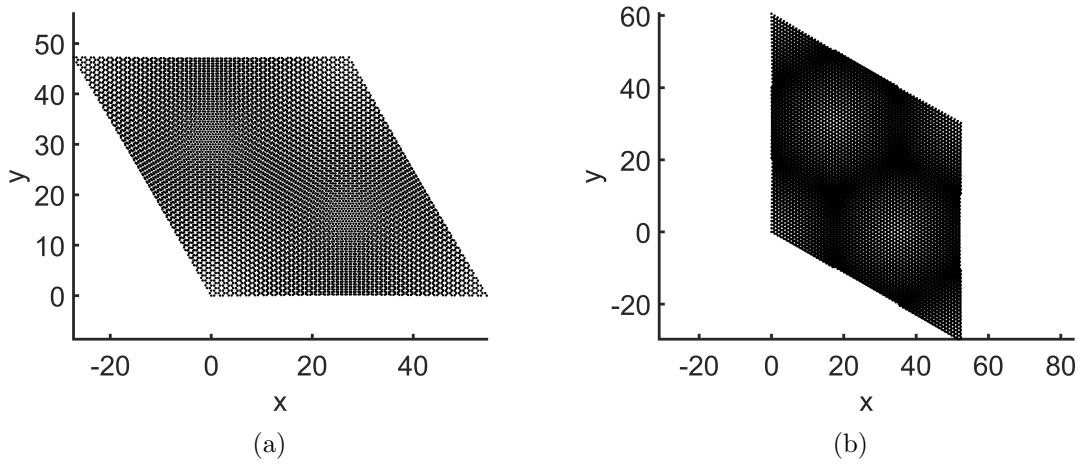


Figure 9: (a) Supercell of moire pattern in TBG with twist angle equal to 1.0501° and corresponding minimum commensurate displacement $\delta_c = a_o$ (b) Supercell of moire pattern in TBG with twist angle equal to 1.6402° and corresponding minimum commensurate displacement $\delta_c = \sqrt{3}a_o$

Using these logics computational codes can be written to simulate the positions of carbons atoms lying inside a supercell of TBG. Figure9 shows the simulated supercell of TBG corresponding to twist angles 1.0501° 9a and 1.6402° 9b. Supercell of TBG corresponding to twist angle 1.0501° contains 2977 lattice points of each of A_1 , B_1 , A_2 and B_2 sublattices. Supercell of TBG corresponding to twist angle 1.6402° contains 3661 lattice points of each of A_1 , B_1 , A_2 and B_2 sublattices.

6. Conclusion

All commensurate moire patterns of TBG can be associated with twist angles laying in range $(0^\circ, 30^\circ)$. If we increase the limit of moire period in the code (code to generate list of commensurate twist angle vs moire period) from $100a_o$ to even larger value then many more commensurate twist angles (lying in range $0^\circ - 30^\circ$) appear in the generated list. By increasing the limit of moire period in the code from $100a_o$ to very large value, so many commensurate twist angles (lying in range $0^\circ - 30^\circ$) can be obtained in the generated list that the difference between any two consecutive values of commensurate twist angles will become very small and the range of commensurate twist

angles will become almost continuous. Therefore, any twist angle can be considered as commensurate twist angle. While characterizing a moire pattern of TBG, corresponding value of minimum commensurate displacement (δ_c) is also important along with corresponding commensurate twist angle. All commensurate moire patterns of TBG can be categorized in two categories: one in which corresponding minimum commensurate displacement is integral multiple of a_o and other in which corresponding minimum commensurate displacement is integral multiple of $\sqrt{3}a_o$. Whenever corresponding minimum commensurate displacement is equal to a_o , the moire pattern of TBG will be perfectly periodic triangular lattice of superlattice points. Whenever corresponding minimum commensurate displacement is different from a_o , the moire pattern of TBG appears to possess strain and rotational symmetry breaking. These defects appear due to presence of similar looking apparent superlattice points along with actual superlattice points in anomalous moire patterns of TBG. Therefore, experimentally observed strain and rotational symmetry breaking in moire pattern of TBG may be due to misunderstanding apparent superlattice points as actual superlattice points. For commensurate twist angles which have very large value of corresponding minimum commensurate displacement in comparison to corresponding actual moire period, the values of apparent moire period will be so small and apparent strain so large that even the commensurate moire patterns of TBG will look like incommensurate moire patterns. Value of apparent moire period decreases with twist angle having a minimum value approximately equal to $1.93185a_o$ corresponding to twist angle equal to 30° . For large values of commensurate twist angles (larger than approximately 25°), the value of apparent moire period becomes so small that commensurate moire patterns of TBG look like incommensurate moire pattern. It is supposed that corresponding to one moire period there corresponds only one commensurate twist angle lying in the interval $(0^\circ, 30^\circ)$, but for some values of actual moire period there corresponds more than one commensurate twist angles lying in the interval $(0^\circ, 30^\circ)$, it might happen for those values of actual moire periods whose corresponding coinciding lattice points, exist on more than one hexagons. There is corrugation in structure of TBG which is caused by varying value of repulsion between two graphene layers at different points of TBG. This repulsion exists among C-C bonds of two graphene layers in TBG. The repulsion between two graphene layers at different points of TBG varies with varying environment of C-C bond of two layers in TBG. Average value of apparent moire period decreases with twist angle and the magnitude of corrugation also decreases with twist angle to minimize stress in C-C bonds of graphene layers of TBG. Using the logics presented in this paper it is possible to write very efficient computational codes to simulate internal configuration of carbon atoms inside a moire supercell of TBG. Using the relationship of apparent strain and apparent moire period with twist angle, the twist angles of fabricated TBG samples can be determined more accurately. Mathematical model to represent corrugation in TBG, presented in this paper, is good enough to represent corrugation of actual TBG samples. Knowledge of the positions of carbon atoms lying inside moire supercell of commensurate twisted bilayer graphene will be very useful to

perform more accurate quantum mechanical calculations related to electronic structure of twisted bilayer graphene, and our computational codes can simulate the internal configuration of carbon atoms inside a supercell of TBG within few minutes even on a laptop with moderate computational power. Taking insight from the description of moire pattern of TBG reported in this paper, the structure of many other types of moire patterns can easily be understood.

Acknowledgments

We acknowledge MHRD India for providing research fellowship and Indian Institute of Technology, Roorkee for providing research facilities.

References

- [1] Lisi S, Lu X, Benschop T, de Jong T A, Stepanov P, Duran J R, Margot F, Cucchi I, Cappelli E, Hunter A, Tamai A, Kandyba V, Giampietri A, Barinov A, Jobst J, Stalman V, Leeuwenhoek M, Watanabe K, Taniguchi T, Rademaker L, van der Molen S J, Allan M P, Efetov D K and Baumberger F 2021 *Nature Physics* **17**(2) 189–193 URL <https://doi.org/10.1038/s41567-020-01041-x>
- [2] Utama M I B, Koch R J, Lee K, Leconte N, Li H, Zhao S, Jiang L, Zhu J, Watanabe K, Taniguchi T, Ashby P D, Weber-Bargioni A, Zettl A, Jozwiak C, Jung J, Rotenberg E, Bostwick A and Wang F 2020 *Nature Physics* **17**(2) 184–188 URL <https://doi.org/10.1038/s41567-020-0974-x>
- [3] Li G, Luican A, Lopes dos Santos J M B, Castro Neto A H, Reina A, Kong J and Andrei E Y 2010 *Nature Physics* **6**(2) 109–113 URL <https://doi.org/10.1038/nphys1463>
- [4] Xie Y, Lian B, Jäck B, Liu X, Chiu C L, Watanabe K, Taniguchi T, Bernevig B A and Yazdani A 2019 *Nature* **572**(7767) 101–105 URL <https://doi.org/10.1038/s41586-019-1422-x>
- [5] Kerelsky A, McGilly L J, Kennes D M, Xian L, Yankowitz M, Chen S, Watanabe K, Taniguchi T, Hone J, Dean C, Rubio A and Pasupathy A N 2019 *Nature* **572**(7767) 95–100 URL <https://doi.org/10.1038/s41586-019-1431-9>
- [6] Cao Y, Fatemi V, Fang S, Watanabe K, Taniguchi T, Kaxiras E and Jarillo-Herrero P 2018 *Nature* **556**(7699) 43–50 URL <https://doi.org/10.1038/nature26160>
- [7] Yankowitz M, Chen S, Polshyn H, Zhang Y, Watanabe K and Taniguchi T G D, Young A F and Dean C R 2019 *Science* **363** 1059–1064 URL <https://www.science.org/doi/abs/10.1126/science.aav1910>
- [8] Oh M, Nuckolls K P, Wong D, Lee R L, Liu X, Watanabe K, Taniguchi T and Yazdani A 2021 *Nature* **600**(7888) 240–245 URL <https://doi.org/10.1038/s41586-021-04121-x>
- [9] Cao Y, Fatemi V, Demir A, Fang S, Tomarken S L, Luo J Y, Sanchez-Yamagishi J D, Watanabe K, Taniguchi T, Kaxiras E, Ashoori R C and Jarillo-Herrero P 2018 *Nature* **556**(7699) 80–86 URL <https://doi.org/10.1038/nature26154>
- [10] Tseng C C, Ma X, Liu Z, Watanabe K, Taniguchi T, Chu J H and Yankowitz M 2022 *Nature Physics* **18**(9) 1038–1042
- [11] Sharpe A L, Fox E J, Barnard A W, Finney J, Watanabe K, Taniguchi T, Kastner M A and Goldhaber-Gordon D 2019 *Science* **365** 605–608 URL <https://www.science.org/doi/abs/10.1126/science.aaw3780>
- [12] Lin J X, Zhang Y H, Morissette E, Wang Z, Liu S, Rhodes D, Watanabe K, Taniguchi T, Hone J and Li J I A 2022 *Science* **375** 437–441 (*Preprint* <https://www.science.org/doi/pdf/10.1126/science.abh2889>) URL <https://www.science.org/doi/abs/10.1126/science.abh2889>
- [13] Benlakhoy N, Jellal A, Bahlouli H and Vogl M 2022 *Phys. Rev. B* **105**(12) 125423 URL <https://link.aps.org/doi/10.1103/PhysRevB.105.125423>

- [14] Choi Y, Kemmer J, Peng Y, Thomson A, Arora H, Polski R, Zhang Y, Zhang Y, Alicea J, Refael G, von Oppen F, Watanabe K, Taniguchi T and Nadj-Perge S 2019 *Nature Physics* **15**(11) 1174–1180 URL <https://doi.org/10.1038/s41567-019-0606-5>
- [15] Jiang Y, Lai X, Watanabe K, Taniguchi T, Haule K, Mao J and Andrei E Y 2019 *Nature* **573**(7772) 91–95 URL <https://doi.org/10.1038/s41586-019-1460-4>
- [16] Lopes dos Santos J M B, Peres N M R and Castro Neto A H 2007 *Phys. Rev. Lett.* **99**(25) 256802 URL <https://link.aps.org/doi/10.1103/PhysRevLett.99.256802>
- [17] Shallcross S, Sharma S, Kandelaki E and Pankratov O A 2010 *Phys. Rev. B* **81**(16) 165105 URL <https://link.aps.org/doi/10.1103/PhysRevB.81.165105>
- [18] Mele E J 2010 *Phys. Rev. B* **81**(16) 161405 URL <https://link.aps.org/doi/10.1103/PhysRevB.81.161405>
- [19] Hasegawa Y and Kohmoto M 2013 *Phys. Rev. B* **88**(12) 125426 URL <https://link.aps.org/doi/10.1103/PhysRevB.88.125426>
- [20] Uchida K, Furuya S, Iwata J I and Oshiyama A 2014 *Phys. Rev. B* **90**(15) URL <https://link.aps.org/doi/10.1103/PhysRevB.90.155451>
- [21] Castro Neto A H, Guinea F, Peres N M R, Novoselov K S and Geim A K 2009 *Rev. Mod. Phys.* **81**(1) 109–162 URL <https://link.aps.org/doi/10.1103/RevModPhys.81.109>
- [22] McCann E and Koshino M 2013 *Reports on Progress in Physics* **76** 056503 URL <https://dx.doi.org/10.1088/0034-4885/76/5/056503>
- [23] Lee J K, Lee S C, Ahn J P, Kim S C, Wilson J I B and John P 2008 *The Journal of Chemical Physics* **129** 234709 (*Preprint* <https://doi.org/10.1063/1.2975333>) URL <https://doi.org/10.1063/1.2975333>
- [24] Lucignano P, Alfè D, Cataudella V, Ninno D and Cantele G 2019 *Phys. Rev. B* **99**(19) 195419 URL <https://link.aps.org/doi/10.1103/PhysRevB.99.195419>
- [25] Fukaya Y, Zhao Y, Kim H W, Ahn J R, Fukidome H and Matsuda I 2021 *Phys. Rev. B* **104**(18) L180202 URL <https://link.aps.org/doi/10.1103/PhysRevB.104.L180202>